Letters in Applied NanoBioScience
Open-Access Journal (ISSN: 2284-6808)

Article
Volume 14, Issue 1, 2025, 21
https://doi.org/10.33263/LIANBS141.021

$CuFe_2O_4$ NPs Mediated Green Synthesis of 5-arylidene Rhodanine Derivatives in Water and their Protective Effects in Terms of Oxidative Stress in Liver, Kidney, and Brain

Abhinav Raj Khandelwal [1], Khushboo Sharma [1], Narsingh Khatik [1], Ravina Meena [1], Renu Bist [2], Sonam Agarwal [3], Harshita Sachdeva [1]

[1] Department of chemistry, University of Rajasthan, Jaipur-302004, Rajasthan, India; abhinavrajkhandelwal09@gmail.com(A.R.K); khushboo.sharma0494@gmail.com (K.S.); narsinghkhatik56@gmail.com (N.K.); ravinameena465@gmail.com (R.M.); drhmsachdevaster@gmail.com (H.S.);
[2] Department of Zoology, University of Rajasthan, Jaipur-302004, Rajasthan, India; renu_bisht22@yahoo.co.in (R.B.);
[3] All India Institute of Medical Sciences, Delhi, India; sonam.2mits@gmail.com (S.A.);
* Correspondence: drhmsachdevaster@gmail.com (H.S.);

Scopus Author ID 6603878358

Received: 13.05.2023; Accepted: 11.08.2023; Published: 24.09.2024

Abstract: A facile, clean, and green protocol for synthesizing 5-arylidene-rhodanine derivatives (3a-3m) by the Knoevenagel condensation of variously substituted aromatic/heteroaromatic aldehydes and rhodanine using $CuFe_2O_4$ NPs as an effective magnetically separable heterogeneous catalyst in water has been developed. Mild reaction conditions, eco-friendliness, higher product yield, recyclability of nanoparticles, and use of water as a green reaction medium are the advantageous features of this environmentally benign protocol. In addition, copper ferrite nanoparticles are synthesized using a green method using *Bougainvillea* glabra flower extract and are characterized by FTIR, UV-visible spectroscopy, SEM, and XRD techniques. Further, the protective effects of 3a and 3b were determined regarding oxidative stress in the liver, kidney, and brain, providing excellent results.

Keywords: $CuFe_2O_4$ nanoparticles; arylidene-rhodanine; Knoevenagel condensation; water; green protocol; oxidative stress.

1. Introduction

Among biologically active heterocyclic nuclei, rhodanine core is the fundamental structural moiety in medicinal chemistry, which exhibits numerous biological activities, viz. insecticidal, anti-diabetic, antibacterial, fungicidal, anti-infective, pesticidal, anti-mycobacterial, antineoplastic, and anthelmintic, etc. [1-10]. Furthermore, rhodanine analogues display anti-tubercular, anti– HIV, and antimalarial activities [11-15]. Besides these activities, rhodanine-based heterocyclic compounds are key in discovering novel drugs. They can be used as antiviral agents against the HHV-6 virus and act as PRL-3 inhibitors, pancreatic lipase inhibitors, PTP1B inhibitors, PRL-3 inhibitors, COX-1/2 and 5-LOX inhibitors, AChE and 15-LOX inhibitors, as potent aldose reductase inhibitors, as a potent stimulator of UCP1 expression to combat obesity, *Mycobacterium tuberculosis* InhA direct inhibitors, *Plasmodium falciparum* Enoyl-Acyl Carrier Protein Reductase inhibitors, potent aldose reductase inhibitors and show peroxisome proliferator-activated receptor γ activity, etc. [16-26]. Zhou *et al*. synthesized the

most potent (*Z*)-2-(5-(4-(dimethylamino) benzylidene)-4-oxo-2-thioxothiazolidin-3-yl)-*N*-phenylacetamide derivative, which exhibits anti-proliferative activity against human cancer cell lines, A549, PC-3, and HepG2. The compound also disrupted cancer A549 cell migration in a concentration-dependent manner [27]. Hence, rhodanine derivatives have attracted the attention of chemists and biologists over the last two decades.

Knoevenagel condensation is the general method of preparing rhodanine derivatives by reacting aromatic aldehydes with 2-thioxo-4-thiazolidinone in the presence of CH_3COOH and CH_3COONa [28]. Other reported methods of Knoevenagel condensation include use of $(CH_3CO)_2O$ [29], urea-rich organic polymer [30], zirconia [31], ionic liquid, acidic alumina, borate zirconia, lipoprotein lipase and I_2/K_2CO_3 as catalysts. Some utilize non-conventional energy sources such as ultrasonication (US) and microwave irradiation (MWI) for synthesizing rhodanine derivatives [32-38].

Gong *et al*. synthesized arylidene-rhodanine derivatives by treating aromatic aldehydes, rhodanine (5mmol), 1-butyl-3-methyl imidazolium hydroxide (basic IL) (0.5 mmol) and H_2O at room temperature [39]. Subhedar *et al*. produced these derivatives in the presence of $[Et_3NH][HSO_4]$ [40] by reacting aldehyde (1mmol), rhodanine/rhodanine acetic acid (1mmol) with IL, $[Et_3NH][HSO_4]$ (20 mol%) at 80°C for 20 min. The Knoevenagel condensation also occurred in the presence of a hydrated ionic liquid (IL), TBAH/H_2O-EtOH [41]. Further, 1,1,3,3-Tetramethylguanidine lactate [TMG][Lac] is also employed as a catalyst for solventless Knoevenagel condensation [42]. The reaction was also performed by utilizing Na_2SO_3 (20 mol %) under reflux in ethanol for 2 hrs [43]. Other catalysts employed for this reaction include morpholine [44], phosphine [45], copper (II) complex functionalized Fe_3O_4 NPs [46], MgO NPs [47], etc. (Table 2).

Even though the reported methods have their benefits and drawbacks in yield, catalyst recovery, product isolation, use of expensive chemicals, etc., there is still room for improvement in terms of environmental impact and cost-effectiveness.

Nowadays, there is increasing concern about environmental protection, and hence, chemical industries are interested in developing safer methods that could reduce waste products from the manufacturing process. Further, the demand for solid acidic and basic catalysts has increased significantly as they give added products in value-added products with excellent yields. In this context, copper and iron-based NPs are popular catalysts for various chemical reactions [48-51].

Among ferrites, spinel ferrites make outstanding catalysts owing to their affordability, recyclability, reusability, and ease of separation from the reaction mixture. Copper ferrite nanoparticles ($CuFe_2O_4$) have emerged as highly effective, green, recyclable heterogeneous catalysts for producing diverse range of medicinally important heterocyclic moieties such as polysubstituted pyrroles, spirooxindoles, benzoxazoles, aminonitriles, 1, 2, 3-triazoles, pyrazolopyridines, spiropyrimidines, aryl and alkyl-14H-dibenzo [aj] xanthenes, triazole-based dihydropyrimidinones, diaryl, alkyl/aryl sulfones, spiropyrazolo pyrimidine derivatives, biscoumarins, naphthoxazinones, chalcone derivatives, and also for the reduction of nitroarenes into amines, etc. [52-71].

Furthermore, research focuses more on utilizing green solvents than organic solvents. Due to easy availability, non-toxicity, non-flammability, and unique property of rate-acceleration via the hydrophobic effect, water provides several benefits as a safe solvent [72, 73]. Previously, we reported lemon juice as a green catalyst to synthesize fluorinated thiazolidinone, pyrazolidinone, and dioxanedione derivatives at room temperature [74].

Herein, we wish to report the production of arylidene rhodanine derivatives in water by employing $CuFe_2O_4$ NPs as a catalyst in continuation to our earlier interest in developing eco-friendly synthetic approaches for synthesizing bioactive heterocyclic compounds [75]. Copper ferrite nanoparticles were prepared from *Bougainvillea* flower extract and characterized using FTIR, UV-visible, SEM, and XRD techniques. -synthesized nanoparticles are more effective than chemically synthesized nanoparticles. Green protocol reduces the harmful effects of traditional methods of NPs synthesis, which is commonly used in research laboratories and industries [76].

Plants are natural chemical industries that do not require any repairs. Plant-assisted nanoparticle synthesis is advantageous in terms of sufficient higher kinetics than other biosynthetic nanoparticle synthesis protocols. Phytochemicals such as aldehydes, amides, flavones, carboxylic acids, terpenoids, phenols, ketones, etc., present in various plant parts have the capability for the reduction of metals salts into respective metal nanoparticles for synthesizing metal-based nanoparticles [77]. Hence, there is a rising need to develop an environment-caring protocol for the synthesis of nanoparticles [78].

The key object of the present investigation is to synthesize copper ferrite nanoparticles using *Bougainvillea glabra* flower extract for its catalytic applications in arylidene rhodanine derivatives. *Bougainvillea glabra* (paper flower or glory of the garden), an ornamental plant, contains constituents such as flavonoids, betacyanins, alkaloids, and tannins. Some species of *Bougainvillea viz. B. buttiana*, *B. glabra*, and *B. spectabilis* are recommended for asthma, bronchitis, respiratory illness, and influenza. It is also effective for the treatment of gastric disorders. Active molecules "pinitol" contained in *Bougainvillea* plant are used for treating diabetes mellitus [79]. Some species of *Bougainvillea* are used to treat ailments such as stomach acidity, diarrhea, leucorrhoea, and hepatitis, and act as an anti-inflammatory, anticancer, antihepatotoxic, antihyperlipidemic, antioxidant, antimicrobial, antibacterial, anti-diabetic, antifertility, antiulcer and antiviral agent [80, 81]. Various types of phytochemicals present in *B. glabra* flowers include tannins, flavonoids, alkaloids, and phenolic compounds. Quercetin is the primary flavonoid constituent in *Bougainvillea* flower extract [82]. Some biologically active rhodanine derivatives are depicted in Figure 1 [83-85].

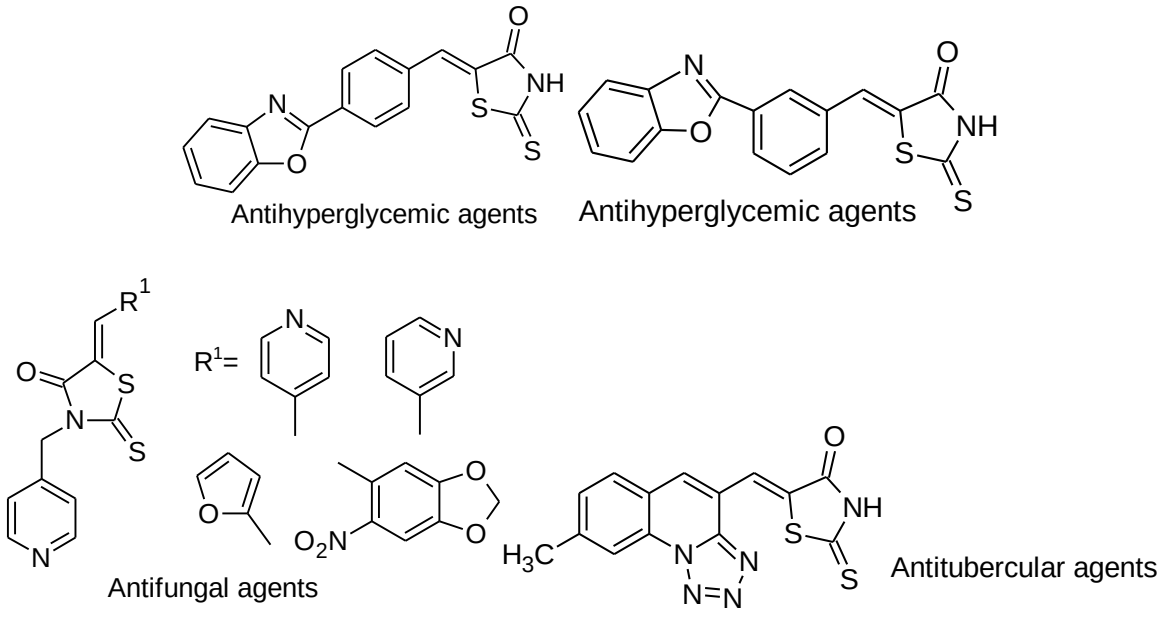

Figure 1. Biologically active rhodanine derivatives.

2. Materials and Methods

2.1. General.

The chemicals used in this study were used as such without additional purification and were purchased from Sigma Aldrich and Merck. The progress of the reaction was checked using thin-layer chromatography (TLC). A melting point apparatus was used to determine melting points, but it was uncorrected. The formed molecules were recognized from their spectral analysis (IR, NMR, and Mass) at SAIF, Punjab University, Chandigarh, and MRC, MNIT, Jaipur. ^{1}HNMR and ^{13}C NMR spectra were recorded on a BRUKER AVANCE NEO at 500MHz spectrometer in DMSO-d_6 using TMS as an internal standard. IR spectra were recorded on Bruker FTIR Alpha Spectrometer. Copper ferrite nanoparticles were characterized using UV-visible, FT-IR, XRD, and SEM analyses. XRD and UV-visible spectra of nanoparticles were measured on PANalytical X'Pert Pro and Thermo Scientific BioMate 3S Spectrophotometer, respectively.

2.2. Synthesis of $CuFe_2O_4$ NPs.

Nanoparticles were prepared in two steps:

2.2.1. Preparation of *Bougainvillea* glabra flower extract.

To remove dust particles, fresh *Bougainvillea* flowers were washed with distilled water and left in sunlight for 8 hours for drying. Dried flowers were ground in a mortar and pestle to obtain fine powder. 10 gm of this fine powder was mixed with de-ionized water (100ml) in a round bottom flask, and the mixture was refluxed for 30 minutes at 60°C. After refluxing, the mixture was filtered to obtain a clear purple solution for *Bougainvillea* flowers. It was then stored for further use in the refrigerator.

2.2.2. Preparation of $CuFe_2O_4$ nanoparticles.

The co-precipitation method was used to prepare NPs. $CuFe_2O_4$ NPs were synthesized by using Cu $(NO_3)_2.3H_2O$ and Fe $(NO_3)_3.9H_2O$ as precursor salts in water by employing *Bougainvillea* flower extract. A solution of Fe $(NO_3)_3.9H_2O$ (0.2 mole) and Cu $(NO_3)_2.3H_2O$ (0.1mole) in water (100 mL) was treated with *Bougainvillea* flower extract (50 ml) at 100°C for 2-3 hours till reddish-black precipitate is obtained. A 1M NaOH solution was added dropwise to the above salt solution to maintain pH 9. Filtration of the formed precipitate was then followed by washing with ethanol. After that, the precipitate was dried and placed in a hot electric oven at 80°C for 24 hrs.

2.2.3. Preparation of 5-arylidine-rhodanine derivatives.

Aromatic/hetero-aromatic aldehydes (10mmol), rhodanine (10mmol), and $CuFe_2O_4$ nanoparticles (20mg) were mixed in 20 ml of H_2O in RB flask and refluxed in an oil bath at 120°C for 30-40 minutes. Reaction progress was checked by TLC (Ethyl acetate: Benzene (1:9) as eluent). As soon as the reaction was completed, the $CuFe_2O_4$ nanoparticles were separated with the help of an external magnet, and the solid product obtained on cooling the mixture was recovered with excellent yield. Further, ethanol was used for the recrystallization of the

products, which were identified by their melting points and spectral data (IR, ^{1}H NMR, ^{13}C NMR) reported in the literature (Table 1) (Scheme 1) [86, 87].

3. Results and Discussion

In continuation of our previous interest in the green synthesis of heterocyclic compounds, herein, we present the synthesis of 5-arylidene-rhodanine derivatives by treating substituted aromatic/heteroaromatic aldehydes with rhodanine in the presence of a catalytic amount of $CuFe_2O_4$ NPs in aqueous media (Scheme-1) (Table 1). The Knoevenagel condensation reaction proceeded smoothly in 30-40 minutes using 20 mg of $CuFe_2O_4$ NPs at 100°C (Table 1). TLC monitored the progress of the reaction. Aromatic aldehydes containing either electron-releasing substituents (ERS) or electron-withdrawing substituents (EWS) reacted well and were converted to corresponding derivatives in 85-95% yield. When the reaction of benzaldehyde with rhodanine was conducted without using any catalyst, only 57% product yield was obtained. Different amounts of $CuFe_2O_4$ NPs (10 mg, 20 mg, and 30 mg) were used to achieve the model reaction. It was observed that 10 mg of catalyst provided only 50-60% yield, while 20 mg of copper ferrite NPs provided 85-95% product yield. No improvement in the yield was observed on further increasing the amount of copper ferrite NPs. Finally, the catalyst's recyclability was tested for forming 3a.

It is further demonstrated that the catalyst can be reused after separating from the reaction mixture for 5 sequential runs without losing its catalytic activity (Figure 6). The synthesized molecules (3a-3m) have been identified by IR, ^{1}HNMR, and ^{13}C NMR spectra and melting points mentioned in the literature (Table 1). The IR spectra of 3a-m showed absorption bands at 3317-3442 cm^{-1} due to amide NH stretching, 1690-1732 cm^{-1} due to -C=O, 1577-1596 cm^{-1} due to C=C, 1152-1229 cm^{-1} due to -C=S stretching which confirms the formation of compounds [41, 74], 3a-m (Figures, 11-15). ^{1}HNMR spectrum of **3b** exhibit following signals (δ_H, ppm): 3.83 (singlet, 3H, OCH_3), 7.11 (d, 2H, Ar-H), 7.57 (d, 2H, Ar-H), 7.60 (s, 1H, =CH), 13.72 (br., 1H, NH); ^{13}C NMR of **3b** shows following signals (δc, ppm): 122.07-132.82 (aromatic carbons), 169.31(-N-C=O), 195.29 (-S-C=S) ppm [41, 74]. The synthesis of nanoparticles takes place in distilled water without using any toxic chemicals. Nanoparticles have also been prepared using *Bougainvillea* flower extract and characterized by XRD, SEM, IR, and UV-Vis Spectroscopy.

We propose the mechanism of this reaction, which involves Knoevenagel-type condensation through Lewis acidic sites of copper ferrite nanoparticles, which coordinates with the oxygen of C=O of the aldehyde group. Activation of rhodanine is followed by C-H bond deprotonation via Lewis basic sites of nanoparticles. Hence, Lewis acidic and basic sites of NPs activated the reactants (Table 1), whereby product formation took place. It is suggested that the reaction occurs by a highly activated copper catalyst, which is intramolecularly coordinated. Furthermore, the spinel binary or ternary oxides provide additional stability and possess exciting features like high strength to resist exceptionally reducing conditions.

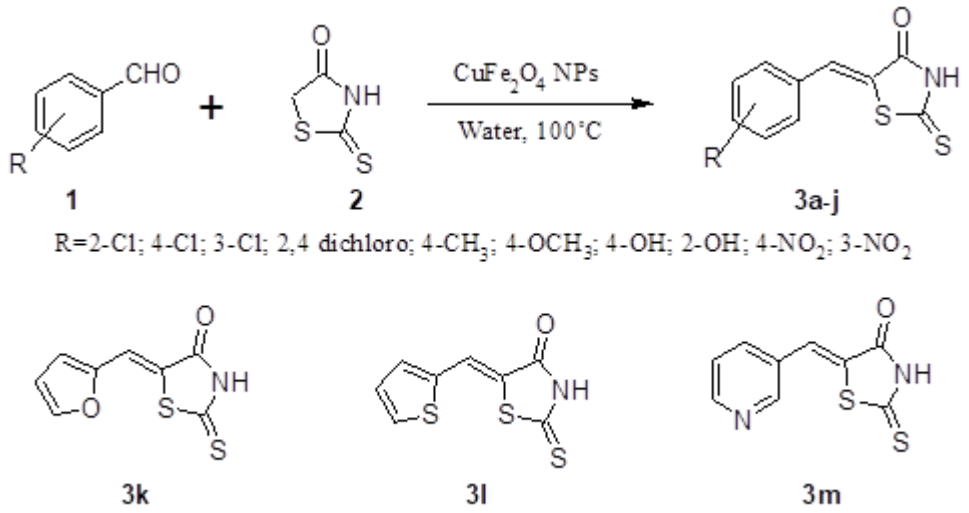

Scheme 1. Formation of 5-arylidene-rhodanine molecules using $CuFe_2O_4$ NPs as an effective catalyst.

Table 1. Experimental data for synthesizing 5-arylidene-rhodanine derivatives (3a-3m) in water.

Entry	Product[a]	Mp (°C)/Ref.	Yield[b] (%)	Time (min.)
3a	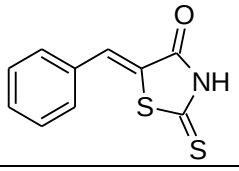	218 [41]	92	30
3b	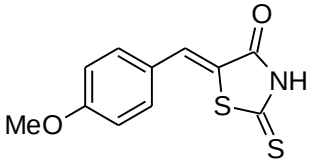	245 [41]	88	40
3c	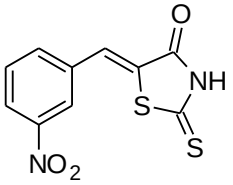	240 [41]	88	35
3d	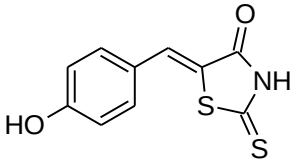	187 [41]	80	30
3e	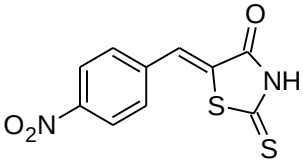	226 [41]	87	25
3f	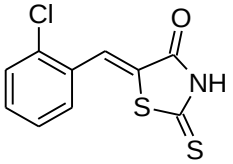	216 [41]	84	40
3g	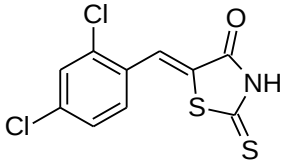	222 [41]	85	30

Entry	Product[a]	Mp (°C)/Ref.	Yield[b] (%)	Time (min.)
3h	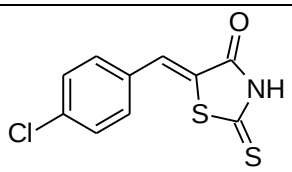	227 [41]	87	40
3i	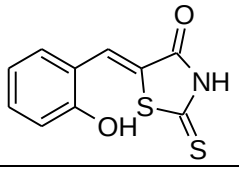	270 [41]	84	35
3j	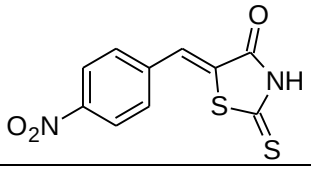	275 [41]	87	40
3k	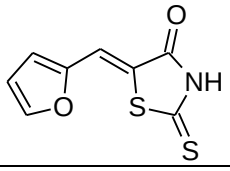	214 [86]	92	35
3l	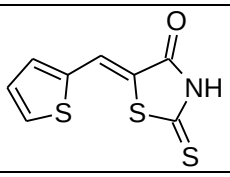	265 [86]	94	25
3m	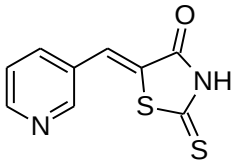	204 [87]	91	30

a Product formation takes place by reacting substituted aromatic/heteroaromatic aldehydes (10mmol) and rhodanine (10mmol) in the presence of $CuFe_2O_4$ nanoparticles (20mg) and water (20mL); **b** Isolated yield of the molecule.

A comparison of catalytic efficiency of copper ferrite nanoparticles with earlier reported methods in terms of the amount of catalyst used, the time required for reaction completion, the yield obtained, and the temperature at which the reaction occurred and solvent used for a particular reaction is presented in Table 2.

Table 2. Previous synthetic approaches for arylidene-rhodanine derivatives.

Name of Catalyst	Amount	Time(hr/min.)	Yield (%)	Solvent	Temp.(°C)	References
TBAH	1 ml	1.5 hr	85-95	EtOH-H_2O	50	41
$[Et_3NH][HSO_4]$	20 mol %	20 min.	84-94	Solvent-free	80	40
[TMG][Lac]	20 mol %	15-30 min.	91-99	Solvent-free	US, 80	42
Titanium Silicate	0.04 gm	30-60 min.	87- 92	Water	90	88
ZnO Nanoparticles	5 mol %	10-26 min	90-99	Ethanol	90	89
Catalyst-free	---	20-35 min.	75-94	Aldonitrones in PEG	80	90
Fe_3O_4@SiO_2-NH_2/Cu(II)	0.15 g	20-60 min.	88-97	Ethanol	Reflux	46
[(*bmim*][OH]	0.5 m mol	10-90 min.	80-98	Water	Room temp.	39
$(NH_4)_2HPO_4$	0.25 mmol	4-18 min.	80-90	Water	90	91
Lemon Juice	2 ml	60-120 min.	90-95	Solvent-free	Room temp.	74
Na_2SO_3	20 mol %	120 min.	70-90	Ethanol	Reflux	43
NEt_3	0.5 m mol	10 min.	45-75	Solvent-free	Room temp.	92
CH_3COONH_4	0.574 g, 0.07 mole	13–25 min	83-97	Solvent-free	Grinding	86

Name of Catalyst	Amount	Time(hr/min.)	Yield (%)	Solvent	Temp.(°C)	References
Morpholine	10 mol%	2 hrs	54-88%	Ethanol	Reflux	44
MgO NPs	30 mol%	45-120 min.	76-95 %	Aqueous ethanol	50	47

3.1. Characterization of copper ferrite nanoparticles.

In the UV-visible spectrum of $CuFe_2O_4$ NPs (Figure 2), higher absorbance is observed at lower wavelengths, which may be due to their smaller size and strong electronic transition of metal ions [93].

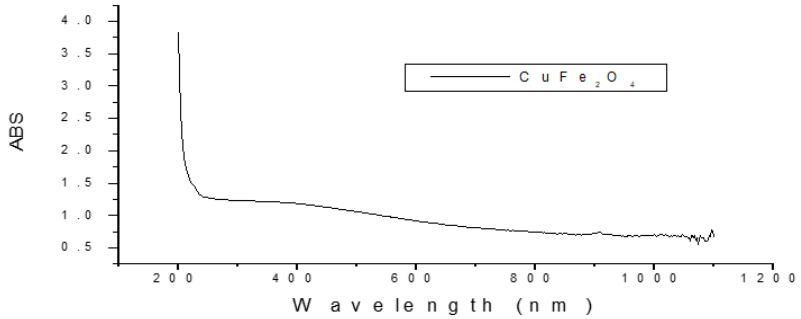

Figure 2. UV–Visible spectra of copper ferrite nanoparticles.

Figure 3 depicts the FT-IR spectrum of spinel $CuFe_2O_4$ NPs prepared from *Bougainvillea* flower extract measured in 400-4000 cm-1, providing valuable evidence regarding its nature and structure. Based on the geometrical configuration of neighboring oxygen atoms, metals in ferrite are present in two different sublattice sites viz. A-site and B-site for tetrahedral and octahedral, respectively. The spectra show two metal-oxygen absorption bands in the 450-300 cm^{-1} and 600-500 cm^{-1} range, which are linked to the vibrations of Cu^{+2}-O^{-2} and Fe^{+3}-O^{-2}, respectively [94]. The absorption bands at 521 cm^{-1} and 435 cm^{-1} are allocated to Fe-O and Cu-O stretching vibrations, respectively. The formation of spinel ferrite material is established by the absorption band at 521 cm^{-1} allocated to Fe-O at the tetrahedral site and 435 cm^{-1} assigned to Cu-O at the octahedral site [95, 96]. A broad band in FT-IR spectra (Figure 3) at 3307 cm^{-1} is allocated to the stretching vibrational mode of water molecules, and it further states that MNPs surface contains O–H groups in large numbers.

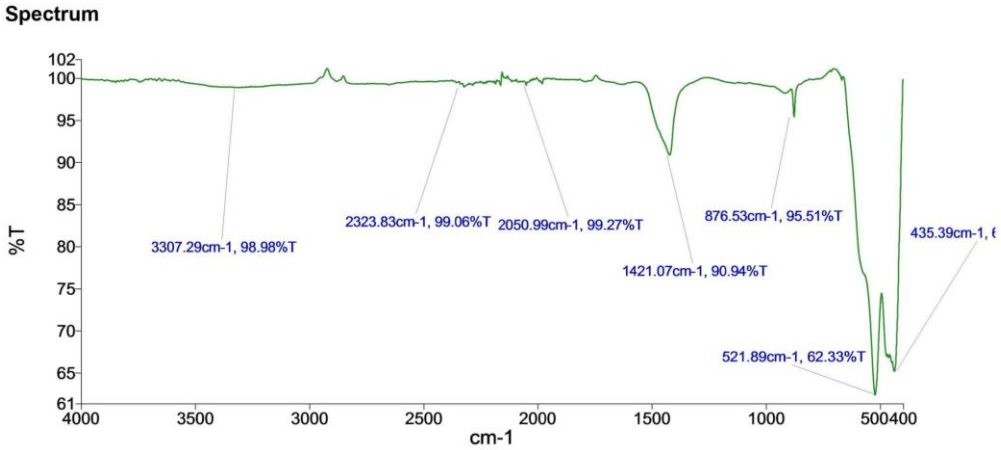

Figure 3. FTIR spectrum of copper ferrite nanoparticles.

The structure, morphology, and size distribution of the prepared $CuFe_2O_4$NPs were examined by SEM (Figure 4). SEM images show high agglomeration in the prepared $CuFe_2O_4$NPs. Further, SEM study suggests that copper ferrite NPs are nanocrystalline, and their shape is irregularly spherical. According to the SEM image, the size of NPs is 200 nm.

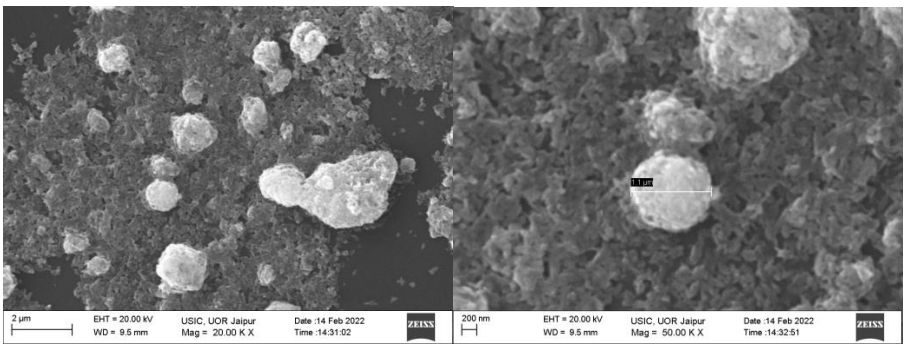

Figure 4. SEM micrograph of the $CuFe_2O_4$ nanoparticles calcined at 500°C for 6 h.

The XRD pattern of the $CuFe_2O_4$-MNPs is depicted in Figure 5. XRD analysis showed a series of diffraction peaks at 2θ of 33.34, 35.74, 38.91, 54.25, 58.35 and 61.75 corresponding to planes (2 2 0), (3 1 1), (4 0 0), (4 2 2), (5 1 1) and (4 4 0) (JCPDF-card no. 01–077-0427), respectively. This XRD pattern agrees with the reported literature, and the spinel structure of $CuFe_2O_4$ nanoparticles is revealed by sharp diffraction peaks [93]. The powder is chiefly comprised of copper ferrite nanoparticles, as indicated by the XRD pattern of calcined nanoparticles [97]. The main diffraction peaks are found between diffraction angle (2θ) = 30–72°, which detects the spinel structure of nano-$CuFe_2O_4$ [93]. We calculated the average size of the nanoparticle from X-ray diffraction by applying the Debye-Scherrer equation:

$D=K \lambda / \beta$ (radians) $\cos \theta = 0.9 \lambda / \beta$ (radians) $\cos \theta$

D= 41.3491+31.219 + 25.697/3=98.2651/3=32.75 nm

B (radians) =FWHM*3.14/180

K is Scherrer constant

Where D is the average crystallite size (nm)

λ is X-ray wavelength, CuKα = 0.15406 nm and θ=Bragg angle in degrees, half of 2θ

B is the line broadening at FWHM in radians

The average size of nanoparticle calcined at 500°C for 6 hrs obtained from the peaks at 2θ= 33.3452, 35.7470, 38.9109 in XRD (Figure 5) using the Scherrer formula is about 32.75 nm.

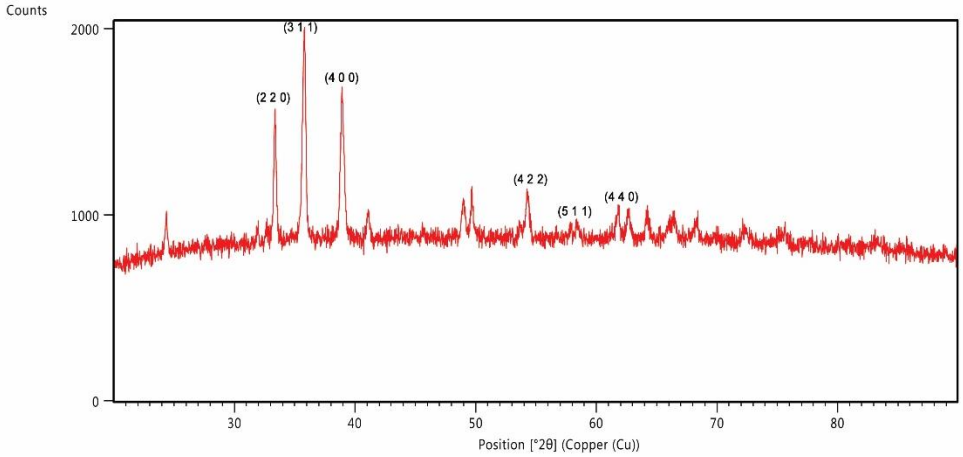

Figure 5. X-ray Diffraction pattern of calcined $CuFe_2O_4$ nanoparticles.

3.2. Regeneration of the catalyst.

One important feature of this methodology is the catalyst's regeneration. The catalyst's recyclability was tested for the formation of 3a. Once the reaction was completed, we

immediately separated and recovered the catalyst with the help of an external magnet, washed it several times with distilled water and acetone, and dried it for further use. The recovered nanoparticles were reused again for five successive runs without losing activity. The isolated yields for successive runs are 90% (I cycle), 88 % (II cycle), 87% (III cycle), 85% (IV cycle), and 83% (V cycle) (Figure 6).

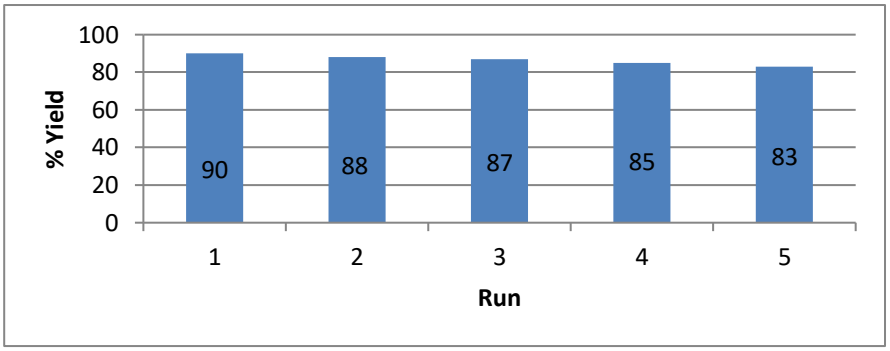

Figure 6. Reusability of $CuFe_2O_4$ with entry 3a, Table 1.

Table 3. Levels of TBARS, PCC, SOD, and CAT in liver, kidney, and brains of differently treated mice.

	Group I (Control)			**Group II (BTT) treated**			**Group III (MBTT) treated**		
Parameters	Liver	Kidney	Brain	Liver	Kidney	Brain	Liver	Kidney	Brain
TBARS (nmole of MDA/ gm of tissue weight	9.88±0.25^{***b}	9.52±0.76^{***b}	11.97±0.23	9.1±0.45^{***a,c}	8.25±0.11	8.45±0.35	8.88±0.65^{**a}	8.1±0.43^{***a}	7.03±0.34
PCC (nmole of carbonyl content/ mg of protein	233.19±0.99	254.09±0.65^{**b}	281.89±0.64	200.88±0.31^{***a,c}	244±0.33^{***a}	270.44±0.54^{***a,c}	210.72±0.29^{***a,b}	242±0.12^{***a}	240.66±1.05^{***a,b}
SOD (µg/mg of protein)	0.048±0.09^{***b}	0.056±0.11	0.062±0.13	0.076±0.02^{***a}	0.088±0.11	0.193±0.32	0.098±0.09	0.102±0.002	0.066±0.01^{***a}
CAT (µmole of H_2O_2 consumed /mg of protein)	162.34±0.52^{***b}	276±0.65	182±0.64^{***b}	184.34±0.44^{***c}	280±0.34	190±0.23^{**a}	254.34±0.52`	298.99±0.65	210.87±0.64^{***a,b}

Expressed Results as mean ± S.E. ***= p< 0.001, **=p< 0.01; **a**= compared to group I, **b**= compared to group II, **c=** compared to group III**;** CAT: Catalase; PCC: Protein carbonyl content; SOD: Superoxide dismutase; TBARS: Thiobarbituric acid reactive substances.

3.3. Determination of Protective Effects of 3a and 3b in liver, brain, and kidney in terms of oxidative stress.

Compounds 3a, (5-benzylidene-2-thiooxothiazolidin-4-one (BTT)) and 3b, 5-(4-methoxybenzylidene)-2-thiooxothiazolidin-4-one (MBTT)) have been evaluated for their protective effects regarding oxidative stress in liver, kidney and brain. The results of levels of TBARS, PCC, SOD, and CAT of differently treated mice are compiled in Table 3 (Figures 7-10). Healthy 6-8-week-old Swiss mice were used for this study. Mice were accommodated and given pelleted food and water *ad libitum*. Mice were used for the experiment after 3-7 days of adaptation. The division of animals was done into 3 groups. Each group contains a minimum of 18 animals [98-101].

3.3.1. Animal care and monitoring.

Healthy Swiss mice, which were 6-8 weeks old (*Mus musculus*), were used for the study. They were obtained from C.C.S. Haryana Agricultural University, Hissar. Mice were accommodated, and a pelleted diet (Hindustan Unilever Limited) and water *ad libitum* were given to them. Mice were used for the experiment after 3-7 days of adaptation. Animals were

maintained and treated according to the Committee for the Purpose of Control and Supervision of Experimentation on Animals (CPCSEA) (Ref. No. BU/BT/383/13-14).

Experimental Design. Division of animals was done into 3 groups with 18 animal's minimum in each group.

GROUPS	TREATMENT	DURATION
Group I	Control (Normal Saline)	72 hours
Group II	5-benzylidene-2-thiooxothiazolidin-4-one (BTT) treated	72 hours
Group III	5-(4-methoxybenzylidene)-2-thiooxothiazolidin-4-one (MBTT) treated	72 hours

3.3.2. Lipid peroxidation (LP).

LP was assayed in terms of TBARS and PCC levels. TBARS was estimated using the method of Ohkawa *et al.*(1979) [98]. Measurement of the amount of malondialdehyde (MDA) formed is carried out by the reaction with thiobarbituric acid at 532nm using a spectrophotometer. Levine *et al*. (1990) [99] provided an established method used for the determination of PCC content.

3.3.3. Superoxide dismutase (SOD).

Dhindsa *et al*. (1981) [100] method was used for the measurement of SOD level. The formazon formation, which is the reaction product of NBT will be read at 540nm.

3.3.4. Catalase (CAT).

Claiborne (1985)[101] method was used to determine the activity of CAT.

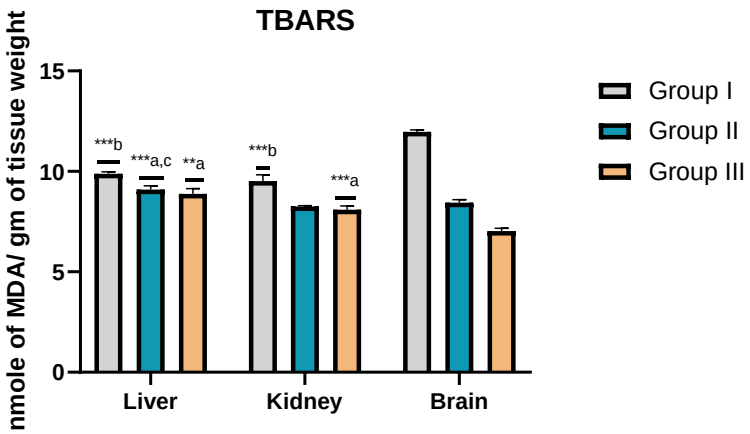

Figure 7. Levels of TBARS in liver, kidney, and brains of differently treated mice. **Group I**: Control; **Group II**: 5-benzylidene-2-thiooxothiazolidin-4-one (BTT) treated; **Group III**: 5-(4- methoxybenzylidene)-2-thiooxothiazolidin-4-one (MBTT) treated; a: compared to group I; b: compared to group II; c: compared to group III; ** P<0.01. ***P<0.001.

The malondialdehyde derivatives (MDA) level was recorded in the differently treated groups' liver, kidney, and brain. In all organs studied, control mice contained the highest level of MDA.

Liver: In liver tissue homogenate, MDA content was significantly elevated compared to group II ($p<0.001$). The mice treated with BTT (group II) exhibited a noteworthy alteration

in MDA activity from groups II and III ($p<0.001$). The minimum level of MDA was found in MBTT-treated mice, and it considerably reduced compared to group I ($p<0.01$).

Kidney: In the kidneys of control mice, the highest MDA level was revealed compared to II and III groups, and it showed a significant alteration from group II ($p.<0.001$). The mice administered with MBTT showed a substantial decline in MDA content compared to the control group ($p.<0.001$).

Brain: In the brains of mice, maximum and minimum MDA levels were recorded for the control group and MBTT MBTT-treated group, respectively.

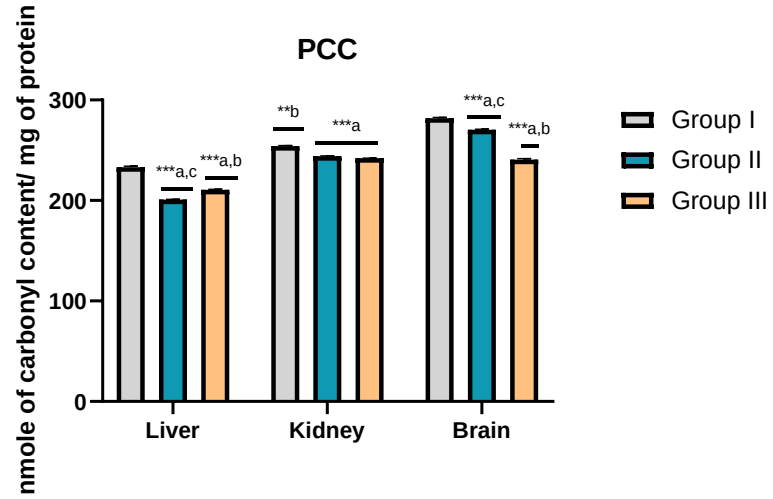

Figure 8. Levels of Protein carbonyl content (PCC) in liver, kidney, and brains of differently treated mice. **Group I**: Control; **Group II**: 5-benzylidene-2-thiooxothiazolidin-4-one **(BTT)** treated; **Group III**: 5-(4-methoxy-benzylidene)-2-thiooxothiazolidin-4-one **(MBTT)** treated a: in comparison to group I; b: in comparison to group II; c: in comparison to group III; ** P<0.01. ***P<0.001.

Liver: The highest PCC in the liver was recorded for control mice, and it was found significantly increased from all the other groups ($p<0.001$). The activity of protein carbonyl moiety was significantly alleviated after BTT treatment as compared to control mice ($p<0.001$), yet it was higher than MBTT-treated mice ($p<0.001$). After the exposure of MBTT, PCC was considerably reduced in comparison with group I ($p<0.001$) but increased in comparison with group II ($p<0.001$).

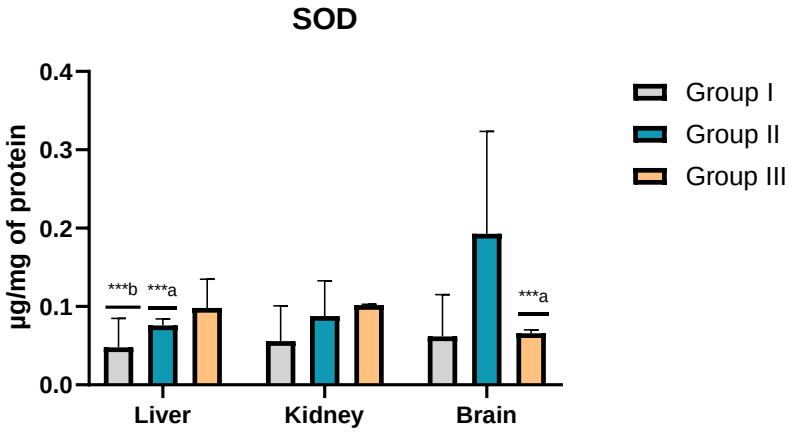

Figure 9. Activities of superoxide dismutase (SOD) in liver, kidney, and brain of differently treated mice. Group I: Control; Group II: 5-benzylidene-2-thiooxothiazolidin-4-one (BTT) treated; Group III: 5-(4-methoxybenzylidene)-2-thiooxothiazolidin-4-one (MBTT) treated; a: compared to group I; b: compared to group II; c: compared to group III; ***P<0.001.

Kidney: In kidneys, maximum PCC was recorded for control mice, and it varied significantly from BTT-treated mice in group II ($P<0.01$). After MBTT treatment, protein carbonyl moieties were reduced compared to groups I ($p<0.001$) and II.

Brain: In the brains of control mice, the maximum level of PCC was recorded among all groups. After administration of BTT in group II, PCC level decreased significantly in control mice, whereas it increased significantly ($p<0.001$) when compared with group III ($p<0.001$). In group III mice, a minimum level of PCC was revealed in brain homogenates in comparison to groups I ($p<0.001$) and II ($p<0.001$).

Liver: Control mice showed minimum SOD activity, whereas after BTT ($p<0.001$) and MBTT treatment, enzymatic activity increased.

Kidney: In the kidneys of control mice, the same pattern of SOD activity was followed as shown in the liver. In control mice, minimum SOD activity was revealed, which, after BTT and MBTT treatment, subsequently increased.

Brain: Control mice showed minimum SOD activity among all groups. In brain homogenates, maximum SOD activities were recorded after BTT administration. After MBTT treatment, activity of SOD alleviated significantly ($p<0.01$) compared to group II.

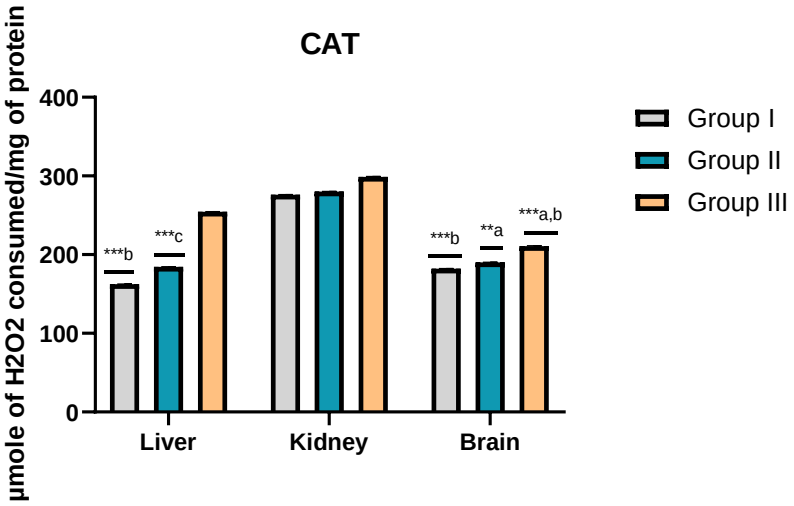

Figure 10. Activities of catalase (CAT) in liver, kidney, and brains of differently treated mice. **Group I**: Control; **Group II**: 5-benzylidene-2-thiooxothiazolidin-4-one (BTT) treated; **Group III**: 5-(4-methoxybenzylidene)-2-thiooxothiazolidin-4-one (MBTT) treated, a: compared to group I; b: compared to group II; c: compared to group III; ** $P<0.01$. ***$P<0.001$.

Liver: A significant difference in CAT activity was observed in control mice as compared to mice treated with BTT ($p<0.001$). In control mice, minimum activity of CAT was observed, which increased subsequently in group II and was found to vary significantly when compared to group III ($p<0.001$). After MBTT treatment, the maximum CAT activity was recorded among all groups.

Kidney: Minimum CAT activity level was recorded in brain homogenates of the control group, which subsequently increased in groups II and III.

Brain: In control mice, CAT activity was found to be minimal among all groups and varied significantly from group II ($p<0.001$). CAT activity increased in group II compared to control mice ($p<0.01$). Further, CAT activity was increased significantly in group III compared to groups I ($p<0.001$) and II ($p<0.001$).

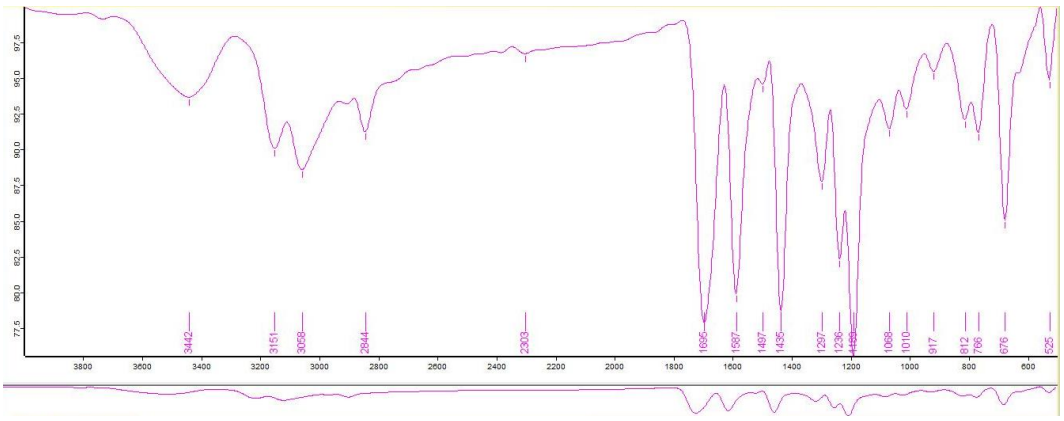

Figure 11. IR Spectra of 5-benzylidene-2-thioxothiazolidin-4-one (3a).

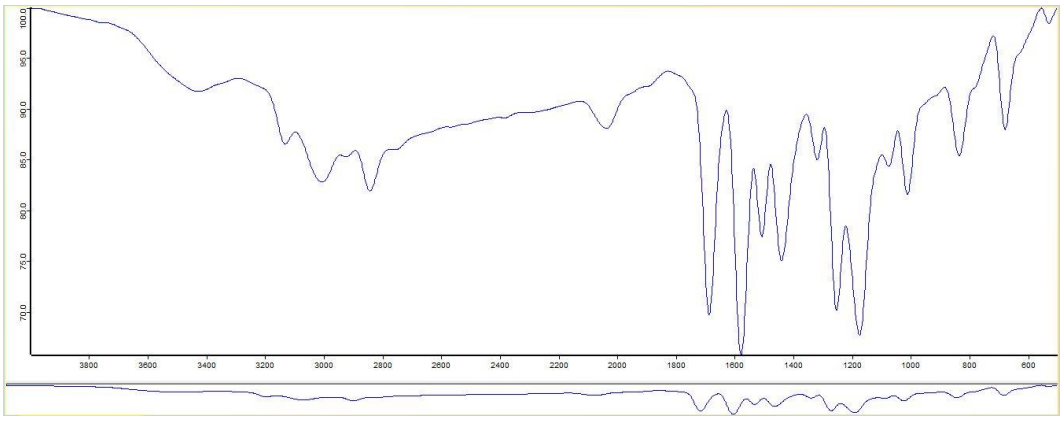

Figure 12. IR Spectra of 5-(4-chlorobenzylidene)-2-thioxothiazolidin-4-one (3h).

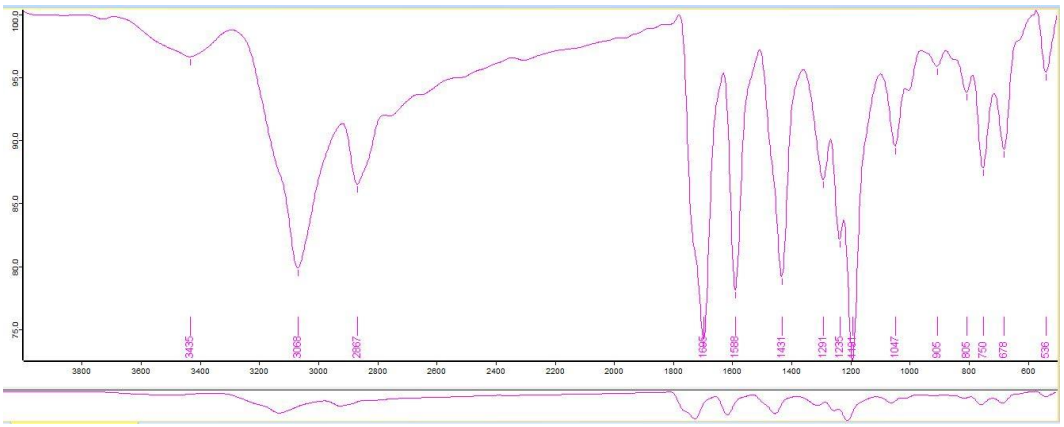

Figure 13. IR Spectra of 5-(2-chlorobenzylidene)-2-thioxothiazolidin-4-one (3f).

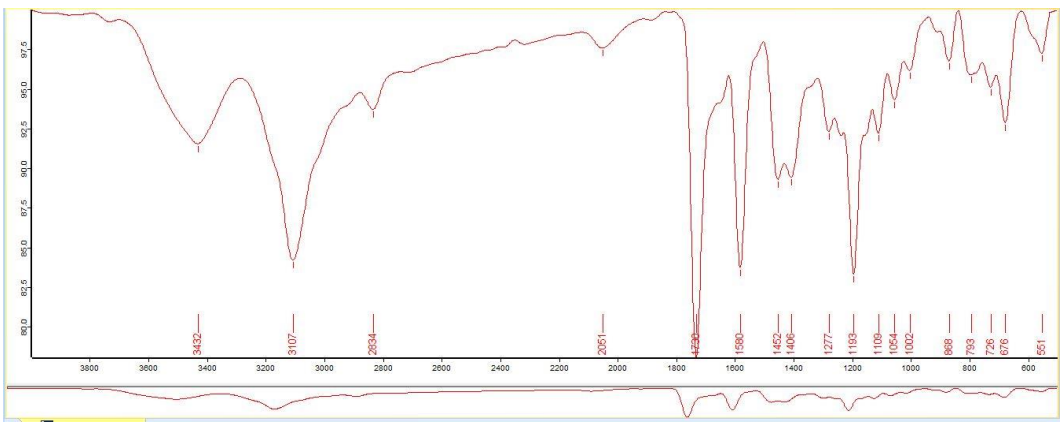

Figure 14. IR Spectra of 5-(2, 4-dichlorobenzylidene) -2-thioxothiazolidin-4-one (3g).

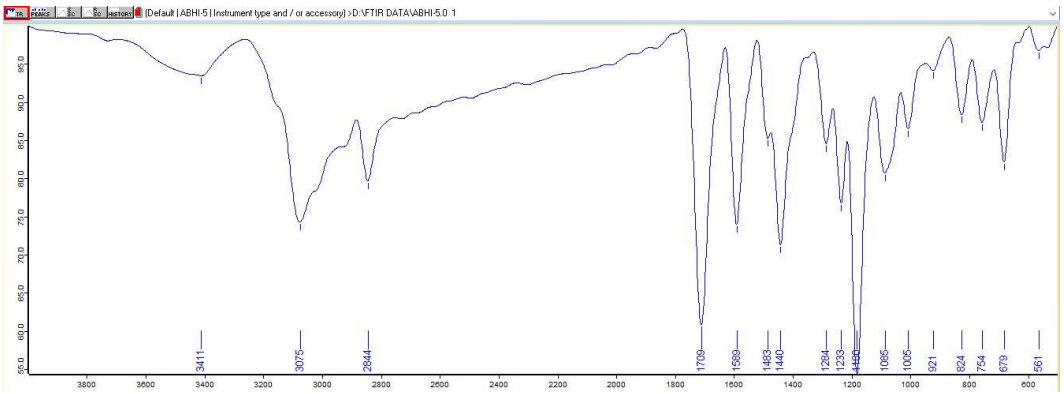

Figure 15. IR Spectra of 5-(4-methoxybenzylidene)-2-thioxothiazolidin-4-one (3b).

4. Conclusions

We have successfully utilized copper ferrite nanoparticles as magnetically recoverable heterogeneous catalysts for the reaction of variously substituted aldehydes with rhodanine. The products were obtained in high yield and short reaction time under mild reaction conditions. Nanoparticles are regenerated and reused five times for the same reaction without losing activity. Moreover, using water as a green solvent makes it a clean and green protocol. Further, the protective effects of 3a and 3b were determined regarding oxidative stress in the liver, kidney, and brain, which offer excellent results.

Funding

Financial support to three authors Mr. Abhinav Raj Khandelwal (File No: 09/149(0813) / 2020-EMR-I), Ms Ravina Meena (File No: 09/149(0804)/2020-EMR-I) and Mr. Narsingh Khatik (File No: 09/149 (0802)/2020-EMR-I) from CSIR, New Delhi is gratefully acknowledged.

Acknowledgments

The authors extend their appreciation to the Head of the Department of Chemistry, Rajasthan University, Jaipur, India, for providing important research facilities in the department. The authors are also thankful to the Director, SAIF, Punjab University, Chandigarh, Manipal University, Jaipur, and MRC, MNIT, Jaipur, for the spectral analyses of the synthesized compounds.

Conflict of Interest

The authors declare that they have no conflict of interest.

References

1. Singh, V.; Singh, A.; Singh, G.; Verma, R. K.; Mall, R. Novel benzoxazole derivatives featuring rhodanine and analogs as antihypergycemic agents: synthesis, molecular docking, and biological studies. *Med. Chem. Res.* **2018**, *27*, 735-743, https://doi.org/10.1007/s00044-017-2097-1.
2. Guo, M.; Zheng, C.-J.; Song, M.-X.; Wu, Y.; Sun, L.-P.; Li, Y.-J.; Liu, Y.; Piao, H.-R. Synthesis and biological evaluation of rhodanine derivatives bearing a quinoline moiety as potent antimicrobial agents. *Bioorg. Med. Chem. Lett.* **2013**, *23*, 4358-4361, https://doi.org/10.1016/j.bmcl.2013.05.082.
3. Chauhan, K.; Sharma, M.; Saxena, J.; Singh, S.V.; Trivedi, P.; Srivastava, K.; Puri, S.K.; Saxena, J.K.; Chaturvedi, V.; Chauhan, P.M.S. Synthesis and biological evaluation of a new class of 4-aminoquinoline–

rhodanine hybrid as potent anti-infective agents. *Eur. J. Med. Chem.* **2013**, *62*, 693-704, https://doi.org/10.1016/j.ejmech.2013.01.017.

4. Toumi, A.; Boudriga, S.; Hamden, K.; Sobeh, M.; Cheurfa, M.; Askri, M.; Knorr, M.; Strohmann, C.; Brieger, L. Synthesis, anti-diabetic activity and molecular docking study of rhodanine-substitued spirooxindole pyrrolidine derivatives as novel α-amylase inhibitors. *Bioorg. Chem.* **2021,** *106*, 104507, https://doi.org/10.1016/j.bioorg.2020.104507.
5. Chaurasyia, A.; Chawla, P.; Monga, V.; Singh, G. Rhodanine derivatives: An insight into the synthetic and medicinal perspectives as antimicrobial and antiviral agents. *Chemical Biology & Drug Design*. **2023**, *101(3)*, 500-549.
6. Maddila, S.; Gorle, S.; Jonnalagadda, S.B. Drug screening of rhodanine derivatives for antibacterial activity. *Expert Opin. Drug Discov.* **2020**, *15*, 203-229, https://doi.org/10.1080/17460441.2020.1696768.
7. Inamori, Y.; Okamoto, Y.; Takegawa, Y.; Tsujibo, H.; Sakagami, Y.; Kumeda, Y.; Shibata, M.; Numata, A. Insecticidal and Antifungal Activities of Aminorhodanine Derivatives. *Biosci. Biotechnol. Biochem.* **1998**, *62*, 1025-1027, https://doi.org/10.1271/bbb.62.1025.
8. Harathi, N.; Sreenivasa Reddy, P.; Sura, M.; Daddam, J.R. Structure prediction, molecular simulations of RmlD from *Mycobacterium tuberculosis*, and interaction studies of Rhodanine derivatives for anti-tuberculosis activity. *J. Mol. Model.* **2021**, *27*, 75, https://doi.org/10.1007/s00894-021-04696-2.
9. Liu, J.; Wu, Y.; Piao, H.; Zhao, X.; Zhang, W.; Wang, Y.; Liu, M. A Comprehensive Review on the Biological and Pharmacological Activities of Rhodanine Based Compounds for Research and Development of Drugs. *Mini Rev. Med. Chem.* **2018**, *18*, 948-961, https://doi.org/10.2174/1389557516666160928162724.
10. Khodair, A.I.; Awad, M.K.; Gesson, J.-P.; Elshaier, Y.A.M.M. New *N*-ribosides and *N*-mannosides of rhodanine derivatives with anticancer activity on leukemia cell line: Design, synthesis, DFT and molecular modelling studies. *Carbohydr. Res.* **2020**, *487*, 107894, https://doi.org/10.1016/j.carres.2019.107894.
11. Ramesh, V.; Rao, B.A.; Sharma. P.; Swarna, B.; Thummuri, D.; Srinivas, K.; Naidu, V.G.M.; Rao, V.J. Synthesis and biological evaluation of new rhodanine analogues bearing 2-chloroquinoline and benzo[h]quinoline scaffolds as anticancer agents. *Eur. J. Med. Chem.* **2014**, *83*, 569-80, https://doi.org/10.1016/j.ejmech.2014.06.013.
12. Tejchman, W.; Kołodziej, P.; Kalinowska-Tłuścik, J.; Nitek, W.; Żuchowski, G.; Bogucka-Kocka, A.; Żesławska, E. Discovery of Cinnamylidene Derivative of Rhodanine with High Anthelmintic Activity against *Rhabditis* sp. *Molecules* **2022**, *27*, 2155, https://doi.org/10.3390/molecules27072155.
13. Mousavi, S.M.; Zarei, M.; Hashemi, S.A.; Babapoor, A.; Amani, A.M. A conceptual review of rhodanine: current applications of antiviral drugs, anticancer and antimicrobial activities. *Artif. Cells, Nanomed. Biotechnol.* **2019**, *47*, 1132-1148, https://doi.org/10.1080/21691401.2019.1573824.
14. Tintori, C.; Iovenitti, G.; Ceresola, E.R.; Ferrarese, R.; Zamperini, C.; Brai, A.; Poli, G.; Dreassi, E.; Cagno, V.; Lembo, D.; Canducci, F.; Botta, M. Rhodanine derivatives as potent anti-HIV and anti-HSV microbicides. *PLoS One* **2018**, *13*, e0198478, https://doi.org/10.1371%2Fjournal.pone.0198478.
15. Yin, L.J.; bin Ahmad Kamar, A.K.D.; Fung, G.T.; Liang, C.T.; Avupati, V.R. Review of anticancer potentials and structure-activity relationships (SAR) of rhodanine derivatives. *Biomed. Pharmacother.* **2022**, *145*, 112406, http://dx.doi.org/10.1016/j.biopha.2021.112406.
16. Zhang, H.-L.; Cui, H.-Y.; Huang, W.-L.; Hu G.-Q. Synthesis and Antitumor Activity of Rhodanine Methylene-Substituted Levofloxacin Derivatives. *Chin. J. Appl. Chem.* **2021**, *38*, 188-194, http://dx.doi.org/10.19894/j.issn.1000-0518.200199.
17. Ahn, J.H.; Kim, S.J.; Park, W.S.; Cho, S.Y.; Du Ha, J.; Kim, S.S.; Kang, S.K.; Jeong, D.G.; Jung, S.-K.; Lee, S.-H.; Kim, H.M.; Park, S.K.; Lee, K.H.; Lee, C.W.; Ryu, S.E.; Choi, J.-K. Synthesis and biological evaluation of rhodanine derivatives as PRL-3 inhibitors. *Bioorg. Med. Chem. Lett.* **2006**, *16*, 2996-2999, https://doi.org/10.1016/j.bmcl.2006.02.060.
18. Chauhan, D.; George, G.; Sridhar, S.N.C.; Bhatia, R.; Paul, A.T.; Monga, V.: Design, synthesis, biological evaluation, and molecular modeling studies of rhodanine derivatives as pancreatic lipase inhibitors. *Arch. Pharm.* **2019**, *352*, 1900029, https://doi.org/10.1002/ardp.201900029.
19. Min, G.; Lee, S.-K.; Kim, H.--N.; Han, Y.-M.; Lee, R.-H.; Jeong, D.G.; Han, D.C.; Kwon, B.-M. Rhodanine-based PRL-3 inhibitors blocked the migration and invasion of metastatic cancer cells. *Bioorg. Med. Chem. Lett.* **2013**, *23*, 3769-3774, https://doi.org/10.1016/j.bmcl.2013.04.092.
20. Liu, H.; Sun, D.; Du, H.; Zheng, C.; Li, J.; Piao, H.; Li, J.; Sun, L. Synthesis and biological evaluation of tryptophan-derived rhodanine derivatives as PTP1B inhibitors and antibacterial agents. *Eur. J. Med. Chem.* **2019**, *172*, 163-173, https://doi.org/10.1016/j.ejmech.2019.03.059.

21. Choi, J.; Ko, Y.; Lee, H.S.; Park, Y.S.; Yang, Y.; Yoon, S. Identification of (β-carboxyethyl)-rhodanine derivatives exhibiting peroxisome proliferator-activated receptor γ activity. *Eur. J. Med. Chem.* **2010**, *45*, 193-202, https://doi.org/10.1016/j.ejmech.2009.09.042.
22. El-Miligy, M.M.M.; Hazzaa, A.A.; El-Messmary, H.; Nassra, R.A.; El-Hawash, S.A.M. New hybrid molecules combining benzothiophene or benzofuran with rhodanine as dual COX-1/2 and 5-LOX inhibitors: Synthesis, biological evaluation and docking study. *Bioorg. Chem.* **2017**, *72*, 102-115, https://doi.org/10.1016/j.bioorg.2017.03.012.
23. Feng, Z.; Wei, Y.; Zhang, Y.; Qiu, Y.; Liu, X.; Su, L.; Liang, N.; Yin, H.; Ding, Q. Identification of a rhodanine derivative BML-260 as a potent stimulator of UCP1 expression. *Theranostics* **2019**, *9*, 3501-3514, https://doi.org/10.7150%2Fthno.31951.
24. Shafii, N.; Khoobi, M.; Amini, M.; Sakhteman, A.; Nadri, H.; Moradi, A.; Emami, S.; Saeedian Moghadam, E.; Foroumadi, A.; Shafiee, A. Synthesis and biological evaluation of 5-benzylidenerhodanine-3-acetic acid derivatives as AChE and 15-LOX inhibitors. *J. Enzyme Inhib. Med. Chem.* **2015**, *30*, 389-395, https://doi.org/10.3109/14756366.2014.940935.
25. Andleeb, H.; Tehseen, Y.; Shah, S.J.A.; Khan, I.; Iqbal, J.; Hameed, S. Identification of novel pyrazole–rhodanine hybrid scaffolds as potent inhibitors of aldose reductase: design, synthesis, biological evaluation and molecular docking analysis. *RSC Adv.* **2016**, *6*, 77688-77700, https://doi.org/10.1039/C6RA14531K.
26. Shaikh, M.S.; Kanhed, A.M.; Chandrasekaran, B.; Palkar, M.B.; Agrawal, N.; Lherbet, C.; Hampannavar, G.A.; Karpoormath, R. Discovery of novel *N*-methyl carbazole tethered rhodanine derivatives as direct inhibitors of *Mycobacterium tuberculosis* InhA. *Bioorg. Med. Chem. Lett.* **2019**, *29*, 2338-2344, https://doi.org/10.1016/j.bmcl.2019.06.015.
27. Zhou, X.; Liu, J.; Meng, J.; Fu, Y.; Wu, Z.; Ouyang, G.; Wang, Z. Discovery of facile amides-functionalized rhodanine-3-acetic acid derivatives as potential anticancer agents by disrupting microtubule dynamics. *J. Enzyme Inhib. Med. Chem.* **2021**, *36*, 1996-2009, https://doi.org/10.1080/14756366.2021.1975695.
28. Brown, F.C.; Bradsher, C.K.; Bond, S.M. Some 5-Arylidene Derivatives. *Ind. Eng. Chem.* **1953**, *45*, 1030–1033, https://doi.org/10.1021/ie50521a047.
29. Ramkumar, K.; Yarovenko, V.N.; Nikitina, A.S.; Zavarzin, I.V.; Krayushkin, M.M.; Kovalenko, L.V.; Esqueda, A.; Odde, S.; Neamati, N. Design, Synthesis and Structure-activity Studies of Rhodanine Derivatives as HIV-1 Integrase Inhibitors. *Molecules* **2010**, *15*, 3958–3992, https://doi.org/10.3390/molecules15063958.
30. Zarei, N.; Yarie, M.; Torabi, M.; Zolfigol, M.A. Urea-rich porous organic polymer as a hydrogen bond catalyst for Knoevenagel condensation reaction and synthesis of 2, 3-dihydroquinazolin-4 (1 H)-ones. *RSC advances* **2024**, *14(2)*, 1094-1105.
31. Reddy, B.M.; Patil, M.K.; Rao, K.N.; Reddy, G.K. An easy-to-use heterogeneous promoted zirconia catalyst for Knoevenagel condensation in liquid phase under solvent-free conditions. Journal of Molecular Catalysis A: Chemical. **2006**, *258(1-2)*, 302-307.
32. Hangarge, R.V.; Jarikote, D.V.; Shingare, M.S. Knoevenagel condensation reactions in an ionic liquid. *Green Chem.* **2002**, *4*, 266–268, https://doi.org/10.1039/B111634G.
33. Shindalkar, S.S.; Madje, B.R.; Shingare, M.S. Microwave induced, solvent-free Knoevenagel condensation of 4-oxo-(*4H*)-1-benzopyran-3-carbaldehyde with Meldrum's acid using alumina support. *Indian J. Chem.* **2006**, *45B*, 2571–2573.
34. Shindalkar, S.S; Madje, B.R.; Hangarge, R.V.; Patil, P.T.; Dongare, M.K.; Shingare, M.S. Bo*rate Zircon*i**a Me***diat***e**d Knoevenagel Condensation Reaction in Water. *J. Korean Chem. Soc.* **2005**, *49*, 377–380, http://doi.org/10.5012/jkcs.2005.49.4.377.
35. Ding, Y.; Ni, X.; Gu, M.; Li, S.; Huang, H.; Hu, Y. Knoevenagel condensation of aromatic aldehydes with active methylene compounds catalyzed by lipoprotein lipase. *Catal. Commun.* **2015**, *64*, 101-104, https://doi.org/10.1016/j.catcom.2015.02.007.
36. Ren, Y.-M.; Cai, C. Knoevenagel Condensation of Aromatic Aldehydes with Active Methylene Compounds Using a Catalytic Amount of Iodine and K_2CO_3 at Room Temperature. *Synth. Commun.* **2007**, *37*, 2209-2213, http://dx.doi.org/10.1002/chin.200801040.
37. Arafa, W.A.A.; Fareed, M.F.; Rabeh, S.A.; Shaker, R.M. Ultrasound mediated green synthesis of rhodanine derivatives: Synthesis, chemical behavior, and antibacterial activity. *Phosphorus Sulfur Silicon Relat. Elem.* **2016**, *191*, 1129-1136, http://dx.doi.org/10.1080/10426507.2016.1146276.
38. Tejchman, W.; Orwat, B.; Korona-Głowniak, I.; Barbasz, A.; Kownacki, I.; Latacz, G.; Handzlik, J.; Żesławska, E.; Malm, A. Highly efficient microwave synthesis of rhodanine and 2-thiohydantoin derivatives

and determination of relationships between their chemical structures and antibacterial activity. *RSC Adv.* **2019**, *9*, 39367-39380, https://doi.org/10.1039/C9RA08690K.

39. Gong, K.; He, Z.-W.; Xu, Y.; Fang, D.; Liu, Z.-L. Green synthesis of 5-benzylidene rhodanine derivatives catalyzed by 1-butyl-3-methyl imidazolium hydroxide in water. *Monatsh. Chem.* **2008**, *139*, 913-915, https://doi.org/10.1007/S00706-008-0871-Y.
40. Subhedar, D.D.; Shaikh, M.H.; Nawale, L.; Yeware, A.; Sarkar, D.; Shingate, B.B. [Et_3NH][HSO_4] catalyzed efficient synthesis of 5-arylidene-rhodanine conjugates and their antitubercular activity. *Res. Chem. Intermed.* **2016**, *42*, 6607-6626, http://dx.doi.org/10.1007%2Fs11164-016-2484-0.
41. Khazaei, A.; Veisi, H.; Safaei, M.; Ahmadian, H. Green synthesis of 5-arylidene-2,4-thiazolidinedione, 5-benzylidene rhodanine and dihydrothiophene derivatives catalyzed by hydrated ionic liquid tetrabutylammonium hydroxide in aqueous medium. *J. Sulfur Chem.* **2014**, *35*, 270-278, https://doi.org/10.1080/17415993.2013.860142.
42. Suresh; Sandhu, J.S. Ultrasound-assisted synthesis of 2,4-thiazolidinedione and rhodanine derivatives catalyzed by task-specific ionic liquid: [TMG] [Lac]. *Org. Med. Chem. Lett.* **2013**, *3*, 2, https://doi.org/10.1186/2191-2858-3-2.
43. Boureghda, C.; Boulcina, R.; Dorcet, V.; Berree, F.; Carboni, B.; Debache, A. Facile synthesis of 5-arylidene rhodanine derivatives using Na_2SO_3 as an eco-friendly catalyst. Access to 2-mercapto-3-aryl-acrylic acids and a benzoxaborole derivative. *Tetrahedron Lett.* **2021**, *62*, 152690, https://doi.org/10.1016/j.tetlet.2020.152690.
44. Jahan, K.; Khan, K.R.; Akhter, K.; Romman, U.K.R.; Halim, E. A convenient approach to synthesize substituted 5-Arylidene-3-*m*-tolyl thiazolidine-2, 4-diones by using morpholine as a catalyst and its theoretical study. *PloS One* **2021**, *16*, e0247619, https://doi.org/10.1371/journal.pone.0247619.
45. Zhang, J.; Zhang, M.; Li, Y.; Liu, S.; Miao, Z. Diastereoselective synthesis of cyclopentene spiro-rhodanines containing three contiguous stereocenters *via* phosphine-catalyzed [3+2] cycloaddition or one-pot sequential [3+ 2]/[3+ 2] cycloaddition. *RSC Adv.* **2016**, *6*, 107984-107993, https://doi.org/10.1039/C6RA23399F.
46. Akhavan, M.; Foroughifar, N.; Pasdar, H.; Khajeh-Amiri, A.; Bekhradnia, A. Copper (II)-complex functionalized magnetite nanoparticles: a highly efficient heterogeneous nanocatalyst for the synthesis of 5-arylidenthiazolidine-2,4-diones and 5-arylidene-2-thioxothiazolidin-4-one. *Trans. Met. Chem.* **2017**, *42*, 543-552, https://doi.org/10.1007/s11243-017-0159-3.
47. Shariati, N.; Baharfar, R. An Efficient One-pot Synthesis of 2-Amino-5-arylidenethiazol-4-ones Catalyzed by MgO Nanoparticles. *J. Chin. Chem. Soc.* **2014**, *61*, 337-340, https://doi.org/10.1002/jccs.201300425.
48. Gawande, M.B.; Goswami, A.; Felpin, F.X.; Asefa, T.; Huang, X.; Silva, R.; Zou, X.; Zboril, R.; Varma, R.S. Cu and Cu- Based Nanoparticles: Synthesis and Applications in Catalysis. *Chem. Rev.* **2016,** *116*, 3722-3811, https://doi.org/10.1021/acs.chemrev.5b00482.
49. Ojha, N.K.; Zyryanov, G.V.; Majee, A.; Charushin, V.N.; Chupakhin, O.N.; Santra, S. Copper nanoparticles as inexpensive and efficient catalyst: A valuable contribution in organic synthesis. *Coord. Chem. Rev*. **2017**, *353*, 1-57, https://doi.org/10.1016/j.ccr.2017.10.004.
50. Poonam; Singh, R. Use of Bimetallic Nanoparticles in the Synthesis of Heterocyclic Molecules. *Curr. Org. Chem.* **2021**, *25*, 351-360, http://dx.doi.org/10.2174/1385272824999200409115018.
51. Sayyahi, S.; Fallah-Mehrjardi, M.; Saghanezhad, S.J. Synthesis of Heterocyclic Compounds by Catalysts Supported on Nano-Magnetite (Fe_3O_4)-An Update. *Mini-Rev. Org. Chem.* **2021**, *18*, 11-26, http://doi.org/10.2174/1570193X17999200507094534.
52. Ganta, R.K.; Ramgopal, A.; Ramesh, C.; Babu, K.R.; Krishna Kumar, M.M.; Rao, B.V. Four-component, one-pot synthesis of spiropyrazolo pyrimidine derivatives by using recyclable nanocopper ferrite catalyst and antibacterial studies. *Synth. Commun.* **2016,** *46*, 1999-2008, http://doi.org/10.1080/00397911.2016.1244271.
53. El-Masry, M.M.; El-Shahat, M.; Ramadan, R.; Abdelhameed, R.M. Selective photocatalytic reduction of nitroarenes into amines based on cobalt/copper ferrite and cobalt-doped copper ferrite nano-photocatalyst. *J. Mater. Sci.: Mater. Electron.* **2021,** *32*, 18408-18424, http://doi.org/10.1007/s10854-021-06387-3.
54. Ghobadi, M. Based on copper ferrite nanoparticles ($CuFe_2O_4$ NPs): Catalysis in synthesis of heterocycles. *J. Synth. Chem.* **2022**, *1*, 84-96, https://doi.org/10.22034/jsc.2022.155234.
55. Satheesh, A.; Usha, H.; Visalakshi, M.; Rambabu, T.; Srinivas, C.V.V.; Vamsi Kumar, Y.; Paul Douglas, S. Nano Copper Ferrite Catalyzed One pot Synthesis and Microbial Studies of Chalcone Derivatives. *Int. J. Eng. Res. Technol.* **2017**, *6*, 1062-1069.

56. Srinivas, B.T.V.; Rawat, V.S.; Konda, K.; Sreedhar, B. Magnetically Separable Copper Ferrite Nanoparticles-Catalyzed Synthesis of Diaryl, Alkyl/Aryl Sulfones from Arylsulfinic Acid Salts and Organohalides/Boronic Acids. *Adv. Synth. Catal.* **2014**, *356*, 805-817, https://doi.org/10.1002/adsc.201301003.
57. Bendi, A.; Dharma Rao, G.B.; Sharma, N.; Tomar, R.; Singh, L. Solvent-Free Synthesis of Glycoside Annulated 1,2,3-Triazole Based Dihydropyrimidinones using Copper Ferrite Nanomaterials as Heterogeneous Catalyst and DFT Studies. *Chemistry Select* **2022**, *7*, e202103910, https://doi.org/10.1002/slct.202103910.
58. Bhaskaruni, S.V.H.S.; Maddila, S.; Gangu, K.K.; Jonnalagadda, S.B. A review on multi-component green synthesis of N-containing heterocycles using mixed oxides as heterogeneous catalysts. *Arab. J. Chem.* **2020**, *13*, 1142-1178, https://doi.org/10.1016/j.arabjc.2017.09.016.
59. Paul, S.; Pal, G.; Das, A.R. Three-component synthesis of a polysubstituted pyrrole core containing heterocyclic scaffolds over magnetically separable nanocrystalline copper ferrite. *RSC Adv.* **2013**, *3*, 8637-8644, https://doi.org/10.1039/C3RA40571K.
60. Bazgir, A.; Hosseini, G.; Ghahremanzadeh, R. Copper Ferrite Nanoparticles: An Efficient and Reusable Nanocatalyst for a Green One-Pot, Three-component Synthesis of Spirooxindoles in Water. *ACS Comb. Sci.* **2013**, *15*, 530-534, https://doi.org/10.1021/co400057h.
61. Yang, D.; Zhu, X.; Wei, W.; Jiang, M.; Zhang, N.; Ren, D.; You, J.; Wang, H. Magnetic Copper Ferrite Nanoparticles: An Inexpensive, Efficient, Recyclable Catalyst for the Synthesis of Substituted Benzoxazoles via Ullmann-Type Coupling under Ligand-Free Conditions. *Synlett* **2014**, *25*, 729-735, https://doi.org/10.1055/s-0033-1340599.
62. Shelke, S.N.; Bankar, S.R.; Mhaske, G.R.; Kadam, S.S.; Murade, D.K.; Bhorkade, S.B.; Rathi, A.K.; Bundaleski, N.; Teodoro, O.M.N.D.; Zboril, R.; Varma, R.S.; Gawande, M.B. Iron Oxide-Supported Copper Oxide Nanoparticles (Nanocat-Fe-CuO): Magnetically Recyclable Catalysts for the Synthesis of Pyrazole Derivatives, 4-Methoxyaniline, and Ullmann-type Condensation Reactions. *ACS Sustainable Chem. Eng.* **2014**, *2*, 1699-1706, https://doi.org/10.1021/sc500160f.
63. Li, Y,; Ning, Y,; Lei, J. Ming T. Ferrite nanocatalysts in the synthesis of heterocycles. *Synthetic Communications* **2021**, *51(10)* 1496-1515. Gharib, A.; Noroozi, Pesyan, N.; Vojdani Fard, L.; Roshani, M. Catalytic Synthesis of α-Aminonitriles Using Nano Copper Ferrite($CuFe_2O_4$) under Green Conditions. *Org. Chem. Int.* **2014,** *2014*, 169803, https://doi.org/10.1155/2014/169803.
64. Bonyasi, R.; Gholinejad, M.; Saadati, F.; Nájera, C. Copper ferrite nanoparticle modified starch as a highly recoverable catalyst for room temperature click chemistry: multicomponent synthesis of 1,2,3-triazoles *in water. New J. Chem. **2018**, 42, 3078*-**3086**, https://doi.org/10.1039/C7NJ03284F.
65. Huang, W.; Jiang, J.; Mandal, T. Ferrite nanoparticles: Catalysis in multicomponent reactions (MCR). *Synth. Commun.* **2021**, *51*, 2397-2422, **h***ttp://*doi.org/10.1080/00397911.2021.1939883.
66. Sarode, S.A.; Bhojane, J.M.; Nagarkar, J.M. An efficient magnetic copper ferrite nanoparticle: for one pot synthesis of 2-substituted benzoxazole via redox reactions. *Tetrahedron Lett.* **2015**, *56*, 206-210, https://doi.org/10.1016/j.tetlet.2014.11.065.
67. Kumar, B.S.P.A.; Reddy, K.H.V.; Satish, G.; Kumar, R.U.; Nageswar, Y.V.D. Synthesis of β-hydroxy-1,4-disubstituted-1,2,3-triazoles catalyzed by copper ferrite nanoparticles in tap water using click chemistry. *RSC Adv.* **2014**, *4*, 60652-60657, https://doi.org/10.1039/C4RA12061B.
68. Sanasi, P.D.; Majji, R.K.; Bandaru, S.; Bassa, S.; Pinninti, S.; Vasamsetty, S.; Korupolu, R.B. Nano Copper Ferrite Catalyzed Sonochemical, One-Pot Three and Four Component Synthesis of Poly Substituted Imidazoles. *Mod. Res. Catal.* **2016**, *5*, 31, https://doi.org/10.4236/mrc.2016.51004.
69. Hassanzadeh-Afruzi, F.; Maleki, A.; Zare, E.N. Novel eco-friendly acacia gum-*grafted*-polyamidoxime@ copper ferrite nanocatalyst for synthesis of pyrazolopyridine derivatives. *J. Nanostruct. Chem.* **2022**, 13, 451-462, http://dx.doi.org/10.1007/s40097-022-00471-8.
70. Bandaru, S.; Majji, R.K.; Bassa, S.; Chilla, P.N.; Yellapragada, R.; Vasamsetty, S.; Jeldi, R.K.; Korupolu, R.B.; Sanasi, P.D. Magnetic Nano Cobalt Ferrite Catalyzed Synthesis of *4H*-Pyrano[3,2-*h*]quinoline Derivatives under Microwave Irradiation. *Green Sustain. Chem.* **2016**, *6*, 101, http://doi.org/10.4236/gsc.2016.62009.
71. Kitanosono, T.; Kobayashi, S. Reactions in Water Involving the "On-Water" Mechanism. *Chem. Eur. J.* **2020**, *26*, 9408-9429, https://doi.org/10.1002/chem.201905482.
72. Hazra, S.; Gallou, F.; Handa, S. Water: An Underestimated Solvent for Amide Bond-Forming Reactions. *ACS Sustainable Chem. Eng.* **2022**, *10*, 5299-5306, https://doi.org/10.1021/acssuschemeng.2c00520.

73. Sachdeva, H.; Dwivedi, D.; Goyal, P. Green Chemical Synthesis and Analgesic Activity of Fluorinated Thiazolidinone, Pyrazolidinone, and Dioxanedione Derivatives. *Org. Chem. Int.* **2013**, *2013*, 976032, https://doi.org/10.1155/2013/976032.
74. Sachdeva, H., Dwivedi, D., Bhattacharjee, R.R., Khaturia, S., Saroj, R.: NiO Nanoparticles: An Efficient Catalyst for the Multicomponent One-Pot Synthesis of Novel Spiro and Condensed Indole Derivatives. *J. Chem.* **2013,** *2013*, 606259, https://doi.org/10.1155/2013/606259.
75. Jamkhande, P.G.; Ghule, N.W.; Bamer, A.H.; Kalaskar, M.G. Metal nanoparticles synthesis: An overview on methods of preparation, advantages and disadvantages, and applications. *J. Drug Deliv. Sci. Technol.* **2019**, *53*, 101174, http://doi.org/10.1016/j.jddst.2019.101174.
76. Rana, A.; Yadav, K.; Jagadevan, S. A comprehensive review on green synthesis of nature-inspired metal nanoparticles: Mechanism, application and toxicity. *J. Clean. Prod.* **2020**, *272*, 122880, http://doi.org/10.1016/j.jclepro.2020.122880.
77. Silva, L.P.; Reis, I.G.; Bonatto, C.C. Green Synthesis of Metal Nanoparticles by Plants: Current Trends and Challenges. In Green Processes for Nanotechnology**,** Basiuk, V.; Basiuk, E., Eds.; Springer, Cham., **2015**, 259-275. http://doi.org/10.1007/978-3-319-15461-9_9.
78. Enciso-Díaz, O.J.; Méndez-Gutiérrez, A.; De Jesús, L.H.; Sharma, A.; Villarreal, M.L.; Taketa, A.C. Antibacterial Activity of *Bougainvillea Glabra*, *Eucalyptus Globulus*, *Gnaphalium Attenuatum*, and Propolis Collected in Mexico. *Pharm. Pharmacol.* **2012**, *3*, 433, http://doi.org/10.4236/pp.2012.34058.
79. Ghogar, A.; Jiraungkoorskul, W. Antifertility Effect of *Bougainvillea* Spectabilis or Paper Flower. *Phcog. Rev.* **2017**, *11*, 19-22, https://doi.org/10.4103%2Fphrev.phrev_44_16.
80. Saleem, H.; Usman, A.; Mahomoodally, M.F.; Ahemad, N. *Bougainvillea glabra* (choisy): A comprehensive review on botany, traditional uses, phytochemistry, pharmacology and toxicity. *J. Ethnopharmacol.* **2021**, *266*, 113356, https://doi.org/10.1016/j.jep.2020.113356.
81. Jadoun, S.; Arif, R.; Jangid, N.K.; Meena, R.K. Green synthesis of nanoparticles using plant extracts: a review. *Environ. Chem. Lett.* **2021**, *19*, 355-374, https://doi.org/10.1007/s10311-020-01074-x.
82. Chauhan, K.; Sharma, M.; Singh, P.; Kumar, V.; Shukla, P.K.; Siddiqi, M.I.; Chauhan, P.M.S. Discovery of a new class of dithiocarbamates and rhodanine scaffolds as potent antifungal agents: synthesis, biology and molecular docking. *Med. Chem. Commun.* **2012**, *3*, 1104-1110, https://doi.org/10.1039/C2MD20109G.
83. Subhedar, D.D.; Shaikh, M.H.; Nawale, L.; Yeware, A.; Sarkar, D.; Khan, F.A.K.; Sangshetti, J.N.; Shingate, B.B. Novel tetrazoloquinoline–rhodanine conjugates: Highly efficient synthesis and biological evaluation. *Bioorg. Med. Chem. Lett.* **2016**, *26*, 2278-2283, https://doi.org/10.1016/j.bmcl.2016.03.045.
84. Matiichuk, Y,; Drapak, I,; Darmograi, N,; Bartoshyk, N,; Drapak, Y,; Matiychuk, V. Synthesis and biological activity of rhodanine-furan conjugates: A review. *Current Chemistry Letters*. **2024,***13(2)*, 287-302..
85. Metwally, N.H.; Rateb, N.M.; Zohdi, H.F. A simple and green procedure for the synthesis of 5-arylidene-4-thiazolidinones by grinding. *Green Chem. Lett. Rev.* **2011**, *4*, 225-228, http://doi.org/10.1080/17518253.2010.544330.
86. Sortino, M.; Delgado, P.; Juárez, S.; Quiroga, J.; Abonía, R.; Insuasty, B.; Nogueras, M.; Rodero, L.; Garibotto, F.M.; Enriz, R.D.; Zacchino, S.A. Synthesis and antifungal activity of (Z)-5-arylidenerhodanines. *Bioorg. Med. Chem.* **2007**, *15*, 484-494, https://doi.org/10.1016/j.bmc.2006.09.038.
87. Gadekar, S.P.; Dipake, S.S.; Gaikwad, S.T.; Lande, M.K. Solid acid TS-1 catalyst: an efficient catalyst in Knoevenagel condensation for the synthesis of 5-arylidene-2,4-thiazolidinediones/Rhodanines in aqueous medium. *Res. Chem. Intermed.* **2018**, *44*, 7509-7518, https://doi.org/10.1007/s11164-018-3570-2.
88. Suresh; Sandhu, J.S. ZnO Nanobelts: An Efficient Catalyst for Synthesis of 5-Arylidine-2,4-Thiazolidinediones and 5-Arylidine-Rhodanines. *Int. J. Org. Chem.* **2012**, *2*, http://doi.org/10.4236/ijoc.2012.223042.
89. Kumar, D.; Narwal, S.; Sandhu, J.S. Catalyst- Free Synthesis of Highly Biologically Active 5-Arylidene Rhodanine and 2,4-Thiazolidinedione Derivatives Using Aldonitrones in Polyethylene Glycol. *Int. J. Med. Chem.* **2013,** *2013*, 273534, https://doi.org/10.1155%2F2013%2F273534.
90. Han, L.; Wu, T.; Zhou, Z. A Simple and Green Procedure for the Synthesis of 5-Arylidenerhodanines Catalyzed by Diammonium Hydrogen Phosphate in Water. *Sci. World J.* **2013,** *2013*, 543768, https://doi.org/10.1155/2013/543768.
91. Sabahi-Agabager, L.; Nasiri, F. One-pot, solvent-free facile stereoselective synthesis of rhodanine–furan hybrids from renewable resources. *J. Sulfur Chem.* **2020**, *41*, 170-181, http://doi.org/10.1080/17415993.2019.1702196.

92. Dave, P.N.; Thakkar, R.; Sirach, R.; Chaturvedi, S. Effect of copper ferrite ($CuFe_2O_4$) in the thermal decomposition of modified nitrotriazolone. *Mater. Adv.* **2022**, *3*, 5019-5026, https://doi.org/10.1039/D2MA00250G.
93. Seyyed Ebrahimi, S.A.; Masoudpanah, S.M. Effects of pH and citric acid content on the structure and magnetic properties of MnZn ferrite nanoparticles synthesized by sol–gel autocombustion method. *J. Magn. Magn. Mater.* **2014**, *357*, 77–81, https://doi.org/10.1016/j.jmmm.2014.01.017.
94. Huang, X., Zhang, J.; Wang, W.; Sang, T.; Song, B.; Zhu, H.; Rao, W.; Wong, C. Effect of pH value on electromagnetic loss properties of Co–Zn ferrite prepared via co-precipitation method. *J. Magn. Magn. Mater.* **2016**, *405*, 36–41, http://doi.org/10.1016/j.jmmm.2015.12.051.
95. Khairy, M.; El-Shaarawy, M.G.; Mousa, M.A. Characterization and super-capacitive properties of nanocrystalline copper ferrite prepared via green and chemical methods. *Mater. Sci. Eng.: B* **2021**, *263*, 114812, https://doi.org/10.1016/j.mseb.2020.114812.
96. Tu, S.; Zhang, Y.; Jia, R.; Jiang, B.; Zhang, J.; Ji, S. A multi-component reaction for the synthesis of N-substituted furo [3,4-*b*]quinoline derivatives under microwave irradiation. *Tetrahedron Lett.* **2006**, *47*, 6521-6525, https://doi.org/10.1016/j.tetlet.2006.07.035.
97. Ohkawa, H.; Ohishi, N.; Yagi, K. Assay for lipid peroxides in animal tissues by thiobarbituric acid reaction. *Anal. Biochem.* **1979,** *95*, 351-358, https://doi.org/10.1016/0003-2697(79)90738-3.
98. Levine, R.L.; Garland, D.; Oliver, C.N.; Amici, A.; Climent, I.; Lenz, A.G.; Ahn, B.W.; Shaltiel, S.; Stadtman, E.R. Determination of carbonyl content in oxidatively modified proteins. *In Methods in enzymology* **1990**, *186*, 464-478.
99. Dhindsa, R.S.; Plumb-Dhindsa, P.; Thorpe, T.A. Leaf Senescence: Correlated with Increased Levels of Membrane Permeability and Lipid Peroxidation, and Decreased Levels of Superoxide Dismutase and Catalase. *J. Exp. Bot.* **1981**, *32*, 93-101, https://doi.org/10.1093/jxb/32.1.93.
100. Tan, D.; Wang, Y.; Bai, B.; Yang, X.; Han, J. Betanin attenuates oxidative stress and inflammatory reaction in kidney of paraquat-treated rat. *Food Chem. Toxicol.* **2015,** *78*, 141-146, https://doi.org/10.1016/j.fct.2015.01.018.